Arch. Metall. Mater. **69** (2024), 1, 25-28

DOI: https://doi.org/10.24425/amm.2024.147778

BUM-SOON PARK[1], JAE-CHEOL PARK[1], HYUN-KUK PARK[1], JEONG-HAN LEE[2*]

MECHANICAL ALLOYING SYNTHESIS AND SPARK PLASMA SINTERING CONSOLIDATION OF Al-Ti-Si-W ALLOYS

Al-Ti-Si-W quaternary powders were mechanically synthesized by planetary ball milling; and further consolidated by spark plasma sintering. The nominal compositions of the quaternary alloys were designed to be $Al_{60}Ti_{30}Si_5W_5$ and $Al_{45}Ti_{40}Si_{10}W_5$ (wt.%). The microstructural evolution of intermetallic compounds in Al-Ti-Si-W alloys included titanium aluminide, titanium silicide, and ternary alloys (Al_xTi_y, Ti_xSi_y, and Ti_xAl_y,Si_z), whereas W was embedded in the Al-Ti matrix as a single phase. The phase composition and grain size distribution were investigated using electron backscatter diffraction analysis, in which refined and uniform microstructures (less than 0.3 μm) were attributed to severe plastic deformation and rapid densification of the pre-alloyed powders. The mechanical properties were correlated with the Al content in the quaternary alloys; a high hardness of 1014.6 ±73.5 kg/mm^2 was observed.

Keywords: Titanium aluminide alloys; mechanical alloying; spark plasma sintering; mechanical property

1. Introduction

Aluminum-titanium (Al-Ti)-based alloys, particularly those containing silicon (Si), are widely used in the aerospace and automotive owing to their excellent lightweight and high strength properties. However, they are difficult to stabilize at high temperatures (>600°C) because of their intrinsic brittleness and workability [1]. To improve the oxidation/corrosion resistance and mechanical properties of Al-Ti-Si ternary system, small amounts (<5 wt.%) of high-melting point elements, such as W, Mo and Ta, are added [2]. In addition, mechanical alloying (MA) is an effective method that utilizes pre-alloyed powders to provide a hardened phase in a ternary system with different physical properties, wherein non-equilibrium phases, including disordered solid solutions and grain-refined nanostructures, are synthesized [3]. Recently, dense grain boundaries (G/Bs) and fine-grained structures have been obtained by spark plasma sintering (SPS) using a high heating rate and pressure. This provides excellent solid-state diffusion routes for the formation of complex TiAl-based intermetallic compounds [4]. However, few studies have been reported on the relationship between intermetallic compounds and dispersion-strengthening effect by adding high melting point elements to Ti-Al-Si ternary materials. In this study, in order to enhance dispersion strengthening and segregation at G/Bs, the effects of W addition on the structural evolution and mechanical properties of Al-Ti-Si ternary alloys are investigated; and the formation and distribution of intermetallic compounds against the strengthening mechanism are discussed.

2. Experimental

Ti (D (0.5): 28.5 μm, >99.95%), Al (D (0.5): 9.1 μm, >99.9%), Si (D (0.5): 20.0 μm, >99.95%), and W (D (0.5): 0.5 μm, >99.5%) powders were used as the starting materials. These powders were mechanically alloyed via high-energy ball milling using stainless steel balls at a ball-to-powder ratio of 2:1. Under a milling time of 9 h and a speed of 300 RPM, the nominal compositions of the alloyed powders were established as $Al_{60}Ti_{30}Si_5W_5$ and $Al_{45}Ti_{40}Si_{10}W_5$. The pre-alloyed powders were sintered by SPS at a sintering temperature of 1000°C and heating rate of 60°C/min under a pressure of 60 MPa. The densification behavior was described by the shrinkage displacement and shrinkage rate as a function of the sintering time and temperature. The phase constitution from the alloyed powder to the consolidated compact was examined through X-ray diffraction (XRD) with CuKα radiation (λ = 0.154 nm). The microstructural evolution with the dispersive distribution of intermetallic

[1] KOREA INSTITUTE OF INDUSTRIAL TECHNOLOGY, AUTOMOTIVE MATERIALS & COMPONENT R&D GROUP, 6, CHEOMDAN-GWAGIRO 208-GIL, BUK-GU, GWANGJU, 61012, KOREA
[2] KOREA INSTITUTE OF INDUSTRIAL TECHNOLOGY, ADVANCED ENERGY MATERIALS AND COMPONENTS R&D GROUP, 33-1, JUNGANG-RO, YANGSAN, GYEONGSANGNAM-DO, 50623, KOREA

* Corresponding author: ljh88@kitech.re.kr

compounds in Al-Ti-Si-W alloys was observed by SEM-EDS. The average grain size and orientation of Al-Ti-Si-W alloys were investigated through EBSD analysis. The average hardness was measured using a Vickers hardness tester with a load of 2 kg applied for 15 s.

3. Results and discussion

Fig. 1 shows the XRD patterns of Al-Ti-Si-W from powder to compact. Most of the raw powders except that of W developed intermetallic compounds with mechanically combined ductile(Al)-brittle(Ti) or brittle(Ti)-brittle(Si) components (see Figs. 1a and 1c) through cold-welding [5]. Metastable solid solutions such as $Ti_xAl_ySi_z$ were substituted with severe plastic deformation (SPD) within the Ti matrix. The structural evolution from powder to compact is shown in Figs. 1c and 1d with magnified major peaks. It is believed that aluminides (TiAl, $TiAl_3$, and Ti_3Al), silicide (Ti_5Si_3), and tau (τ: $Ti_{1.1}Al_{2.4}Si_{0.5}$) phases are formed through SPD with significant distortion within the lattice during the densification for inter-diffusion. As G/B migrations after neck formation in agglomerated inter-particles were established, the lattice parameter of each intermetallic compound decreased while releasing distorted compressive stress, e.g. 2.241 (Ti_xAl_y) → 2.222 Å (TiAl), ε: 0.09 → 0.14 (see Fig. 1c) and 2.345 (Ti_xAl_y) → 2.311 Å (TiAl), ε: 0.11 → 0.25 (see Fig. 1d). In a concentrated solid solution, the elastic modulus and lattice mismatch (distortion) are the major factors contributing to the strengthening; it is considered that SPD in the lattice (in the powder state) induced by MA eventually causes solid solution strengthening (in the compact state).

Fig. 2 shows field emission scanning electron microscopy (FE-SEM) images of Al-Ti-Si-W alloys after sintering at 1,000°C. The microstructures of Al-Ti-Si-W are composed of aluminides (TiAl, light grey, $TiAl_3$, dark grey), silicide (Ti_5Si_3, black), and W-inclusions (white) with the fine-grained structure $Ti_{1.1}Al_{2.4}Si_{0.5}$ in a Ti(Al, Si) matrix. These intermetallic compounds were confirmed to be consistent with the result of the quantitative analysis at each point (1-4). In the Al-rich corner, the Ti(Al, Si) solid solution formed phase owing to the inter-diffusion of the Ti/Al interface while melting to the liquid state (L), terminating at 579°C, i.e. (Al) + (Ti) → L + τ [6]. The Ti-rich corner, the (α-Ti) was formed after decomposing into each intermetallic compound corresponding to an invariant reaction of up to 1,035°C, i.e. (α-Ti) → Ti_3Al (α_2) + TiAl (γ) + Ti_5Si_3 (ζ) [6]. On the other hand, the formation of a thermodynamically unfavorable $TiAl_3$ phase is correlated with a mismatch of the Ti/Al interface through an excess of the unconsumed Al corner after the formation of the phase. Owing to rapid densification (700-1,000°C), the quasi-liquid Al corner rapidly reacts with the Ti core, such as a type of recrystallization while hindering direct contact with other intermetallic compounds.

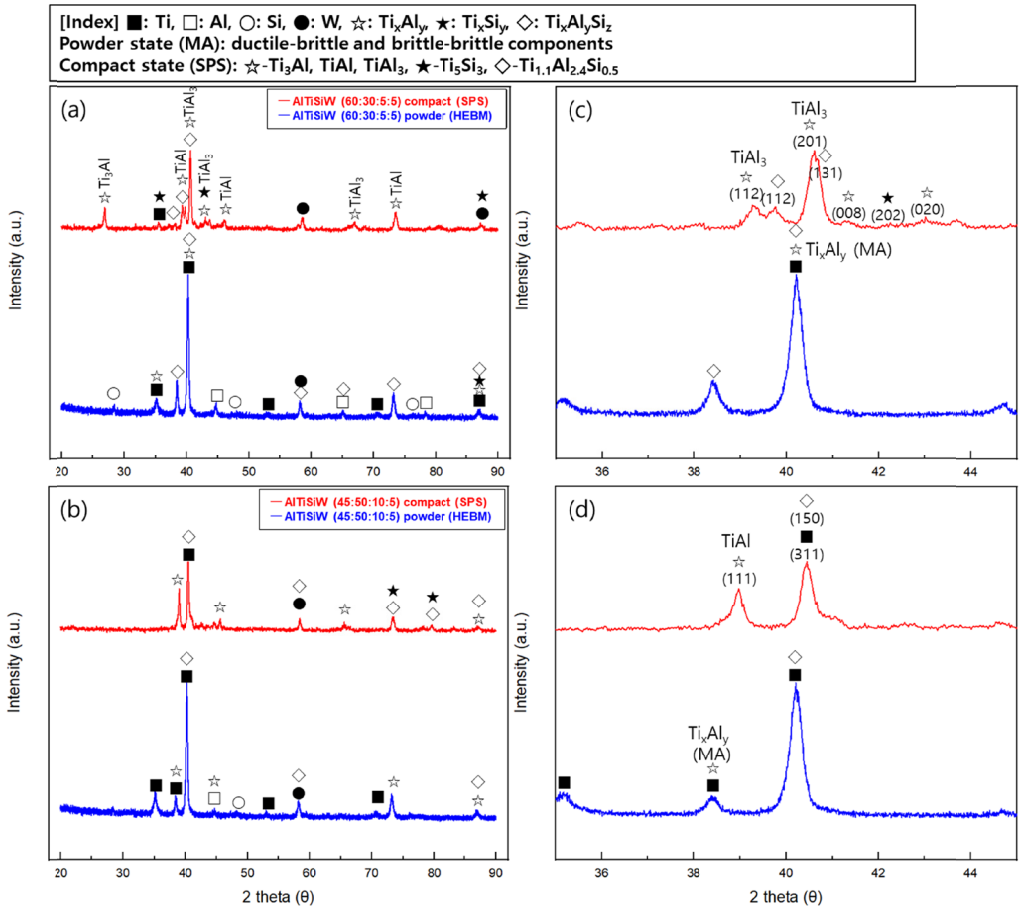

Fig. 1. XRD patterns of Al-Ti-Si-W alloys fabricated by high energy ball milling and spark plasma sintering: (a) $Al_{60}Ti_{30}Si_5W_5$, (b) $Al_{45}Ti_{50}Si_{10}W_5$, (c) and (d) magnification of peaks for major phases

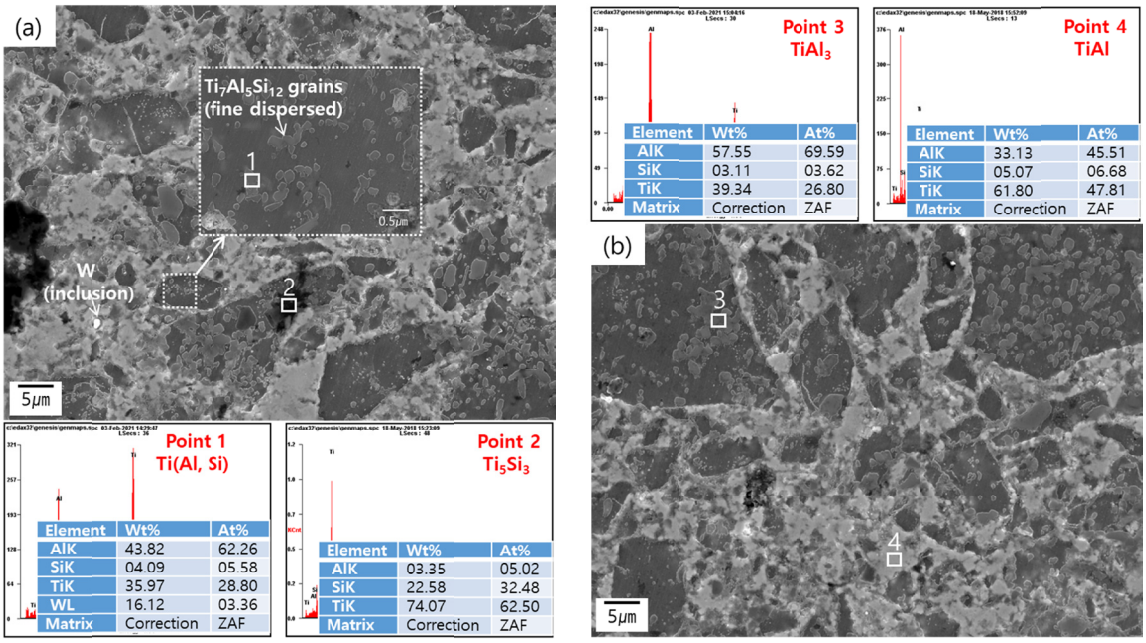

Fig. 2. Microstructure and quantitative analysis of Al-Ti-Si-W alloys showing different of the phase constituents (a) $Al_{60}Ti_{30}Si_5W_5$ and (b) $Al_{45}Ti_{40}Si_{10}W_5$

Fig. 3 shows the EBSD results of Al-Ti-Si-W alloys to investigate the exact phase identification and distribution. In the Al-rich composition (see Fig. 3b), fine grains with many inhomogeneous G/Bs due to the recrystallization of $TiAl_3$, resulting in a wide grain size distribution (min: 0.1; max: 2.3; mean: 0.6 (μm)) were observed. It was attributed that a minority of

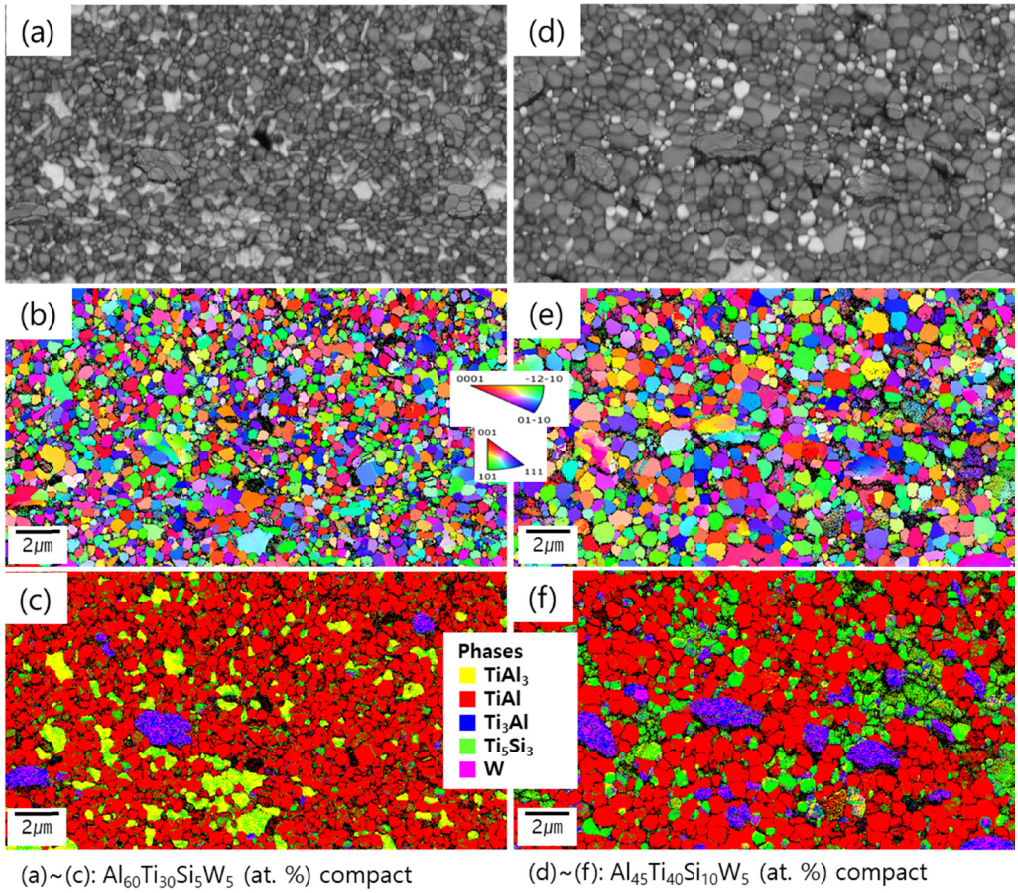

Fig. 3. EBSD analysis of Al-Ti-Si-W alloys: (a), (d) band contrast images, (b), (e) grain orientation maps with inverse pole figure, and (c), (f) phase distribution

G/Bs inducing non-equilibrium faceting for mismatched interfaces (between intermetallic compounds) controlled structural evolution with localization of deformation caused by SPD [7]. On the other hand, as seen in Fig. 3e, relatively uniform G/B and size were confirmed due to the dominant distribution (min: 0.3; max: 1.2; mean: 0.5 (μm)) of thermodynamically stable phases; i.e, TiAl and Ti_5Si_3. For a detailed comparison of the phase distributions, color maps are shown in Figs. 3c and 3f. The five color areas depict each intermetallic compound, namely yellow ($TiAl_3$), red (TiAl), blue (Ti_3Al), green (Ti_5Si_3), and magenta (W). Comparing the area fractions of $TiAl_3$ and Ti_5Si_3 phases, it is clear that $TiAl_3$ occupies a large fraction in the Al-rich corner (see Fig. 3c, $TiAl_3$: 0.216), whereas Ti_5Si_3 is formed in the Ti-rich corner (see Fig. 3f, Ti_5Si_3: 0.241), which is consistent with the aforementioned formation of the main intermetallic compounds at the phase interfaces.

Fig. 4 shows the hardness values of the Al-Ti-Si-W alloy with those reported in previous studies. In particular, high hardness values were exhibited despite the composition dominated by Al-rich corner due to the strengthening mechanisms. Average hardness values were 977.0 MPa (996.2 kg/mm^2) and 995.0 MPa (1014.6 kg/mm^2) according to the Al content in Al-Ti-Si-W alloys. The $Al_{45}Ti_{40}Si_{10}W_5$ alloy achieves the highest hardness (1088.0 kg/mm^2) owing to the formation of a higher amount of silicide than aluminides against Si substitution in the Ti-Al matrix (e.g. Young's modulus; Ti_5Si_3: 222-253 GPa, $TiAl_3$: 202-215 [1]). Additional hardening factors to be considered are: (i) discontinuous precipitation-hardening by (W) in the aluminide interface during the densification; (ii) grain refinement of the tau phase (brittle) by recrystallization of $TiAl_3$, while hindering the growth of the Ti core; and (iii) active and fast inter-diffusion with hardened G/Bs by rapid sintering.

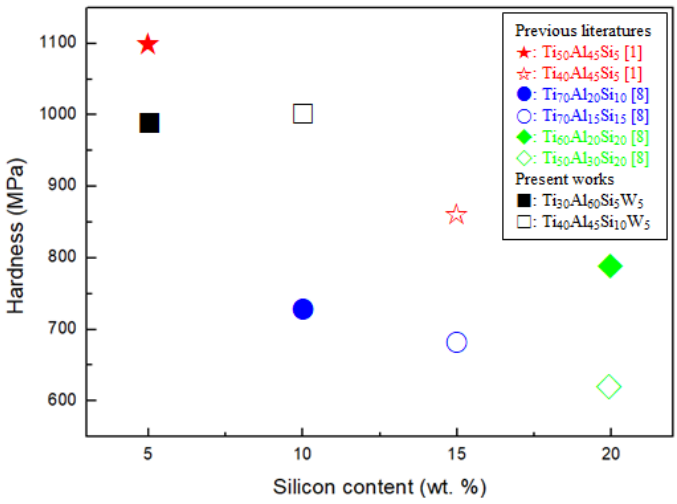

Fig. 4. The comparison of Al-Ti-Si based alloys hardness values of present and the literature studies

4. Conclusions

This study concludes the following regarding the effect of the MA and SPS methods on the transformation of Al-Ti-Si-W alloy from the powder to a compact state.

1. Solid-solution strengthening in Al-Ti-Si-W alloy powders caused compressive stress in the lattice distortion caused by SPD.
2. The microstructure of Al-Ti-Si-W alloy consisted of TiAl, $TiAl_3$, Ti_3Al, $Ti_{1.1}Al_{2.4}Si_{0.5}$, and Ti_5Si phases, and the distribution and grain size of the intermetallic compounds according to the alloy composition were also discussed.
3. The discontinuous dispersion-strengthening by tungsten (W) precipitate in aluminides interface and grain refinement of tau phase by recrystallization of $TiAl_3$ were effected hardening fine nanograined of aluminides and silicides.

Acknowledgments

This study has been conducted with the support of the Korea Institute of Industrial Technology as "Development of core technologies of AI based self-power generation and charging for next-generation mobility (KITECH EH-23-0013)".

REFERENCES

[1] J.H. Lee, H.K. Park, J.H. Kim, J.H. Jang, S.K. Hong, I.H. Oh, J. Mater. Res. Technol. **9** (2), 2247-2258 (2020).

[2] D.V. Shtansky, A.N. Sheveiko, M.I. Petrzhik, F.V. Kiryukhantsev-Korneev, E.A. Levashov, A. Leyland, A.L. Yerokhin, A. Matthews, Surf. Coat. Technol. **200**, 208-212 (2005).

[3] S.H. Noh, T.K. Kim, J. Korean Powder Metall. Inst. **28** (5), 375-380 (2021).

[4] L.R. Kanyane, A.P. Popoola, N. Malatji, Results Phys. **12**, 1754-1761 (2019).

[5] C. Suryanarayana, Research, 4219812 (2019).

[6] S.A. Raji, A.P.I. Popoola, S.L. Pityana, O.M. Popoola, Heliyon **6**, e04463 (2020).

[7] X. Sauvage, G. Wilde, S.V. Divinski, Z. Horita, R.Z. Valiev, Mater. Sci. Eng. A, **540**, 1-12 (2012).

[8] A. Knaislova, P. Novak, M. Cabibbo, F. Prusa, C. Paoletti, L. Jaworska, D. Vojtech, J. Alloys Compd. **752**, 317-326 (2018).